Real-time electric vehicle mass identification

Erik Wilhelm[1], Lennon Rodgers[2], Raffaele Bornatico[3]

[1]*Singapore University of Technology and Design, Singapore, erikwilhelm@sutd.edu.sg*
[2]*Massachusetts Institute of Technology, USA*
[3]*ETH-Zurich, Switzerland*

Abstract

A technique capable of identifying electric vehicle (EV) mass in real-time has been a topic of research for several years due to the advantages it presents, such as the ability to dramatically improve range estimates, perform more effective torque vectoring for ABS/ESC, track delivery vehicle weight, etc.. Some crucial issues in mass identification impede an easy implementation of such an algorithm, however, and this work introduces a simple method to calculate EV mass on-the-fly using standard data available on most CAN buses and therefore without the need of additional sensors. The results presented here are achieved using an eight step technique suitable for accurate mass estimations during wide-open-throttle acceleration events. The algorithm's instantaneous error is less than 10%, and converges to better than 3% absolute accuracy performance with subsequent measurements. A preliminary analysis of trips lacking hard acceleration presented in this paper show an inability to differentiate between loaded and unloaded conditions.

Keywords: modeling & simulation, real-time, mass identification, electric vehicles

1 Introduction

Much attention has been given to the problem of identifying vehicle loss parameters, particularly vehicle mass. Notable previous work has attempted to fit parameters from linear dynamics and powertrain models using least-squares [1], [2] and more exotic and complicated methods [3], [4]. This work extends previous work presented by the authors pushing the state-of-the-art of identifying electric vehicle mass in real-time [5]. The streamlined approach sacrifices some accuracy for computational efficiency, but by collecting large volumes of data the algorithm converges to reasonable estimates. The methods presented can be used to increase the accuracy of electric vehicle distance-to-empty estimates, improve ABS/ESC control performance, enable fleet managers to have greater insight into the current state of their fleet, as well as to enable car sharing agencies to track customer usage to provide a higher level of service.

Figure1: The Mitsubishi iMiEV test vehicle

The test vehicle used in this work is a 2011 Mitsubishi iMiEV, similar to the vehicle shown in Figure 1. The manufacturer's specifications for the test vehicle are summarized in Table 1.

Table 1: Physical characteristics of the test vehicle

Curb weight	1120 kg
Battery capacity	16 kWh
Battery chemistry	Li-Ion
Maximum range	100 km (US EPA)
Maximum speed	130 km/h
Motor Power (peak)	47 kW
Motor efficiency (mean)	80%
Motor Torque (peak)	180 N-m
Tires	P145/65R15 BSW

2 Methods

The strength of the approach presented in this paper is its dependence on minimal amounts of data. In theory, only motor power and vehicle speed signals are required to perform the mass identification. In practice, however, three signals are required because of how the vehicle's CAN bus is structured: motor current (A), motor voltage (V), and vehicle speed (km/h) are used.

A simple but effective algorithm for determining vehicle mass in real-time using CAN parameters was developed, and proceeds by:

1. Calculating power and acceleration from P=I·V and $\ddot{x} = \frac{dv}{dt}$,
2. smoothing the data using a rolling average of N samples (where N is often heuristically chosen to be between 20-50 for power, and between 5-10 for acceleration),
3. finding events where power demand is positive and stable (within +/- 3.5 kW bounds) for a period of N*=10 samples,
4. checking that the velocity/acceleration signals are consistent with the constant torque events (within +3 and 0.5 m/s² bounds) for a period of N*=20 samples,
5. and, if the torque and acceleration data has reached steady state over a common period in the trip,
6. the force F_{trac} applied to road from motor power and gear ratio is calculated using Equation 1 (where

motor torque τ is multiplied by gear ratio and divided by the radius of the wheel r_w),
7. and finally by the calculating of mass m_{ident} using Equation 2 (Newton's second law),
8. The identified masses are checked for compliance with physical parameter limits outlined in Table 2.

$$F_{trac} = \frac{\tau \cdot G}{r_w} \qquad (1)$$

$$m_{ident} = \frac{F_{trac}}{\ddot{x}} \qquad (2)$$

It is assumed that the drivetrain efficiency retains the constant value given outlined in Table 1, which surprisingly does not corrupt the accuracy of the mass measurement.

To account for the 'apparent mass' which is impedes acceleration, the equivalent mass of the vehicle m_{equiv} is used throughout this work and is reported simply as mass in all of the results. This mass, calculated in Equation 3, is due to the inertial forces imbued by rotating parts (tires, motor etc.) and is a factor which increases the vehicle's apparent curb weight. The fixed gear reduction coefficient G has a value of 7.6 which was calculated from comparing measured vehicle speed and motor RPM. This equation makes several simplifications, and its heuristic assumptions are discussed in detail in [6], [7].

$$m_{equiv} = m \cdot (1 + 0.04 + 0.0025 \cdot G^2) \qquad (3)$$

In order to examine how the mass estimate settles to a value under different test conditions (i.e. different passenger configurations), the cumulative mean for the test run m_{cum} is calculated using Equation 4.

$$m_{cum}(n) = \frac{1}{n} \sum_{k=0}^{n} m_{ident}(k) \qquad (4)$$

The parsing of the mass estimates in step 8 of the algorithm is performed using the conditions of physical realizability in Table 2. It is important to note that these conditions exceed manufacturer specifications in all cases except for mass bounds, which are held at the Gross Vehicle Mass which the manufacturer specifies.

Table 2: Physical limits used to parse mass estimates

Parameter	Max	Min
Acceleration (m/s2)	2.7	0
Power (kW)	60	0
Torque (N-m)	220	0
Mass (kg)	1520	1125
Apparent mass (kg)	(1958)	(1450)

Throughout the following section, the data for which results will be discussed come from two main trials, and are labeled as such:

A) Controlled on-road tests under wide-open-throttle conditions with
    i.   Driver only
    ii.   Driver and one passenger
B) Real-world driving with
    i.   Driver only
    ii.   Full vehicle (3 passengers)

The source code used to generate the results in the following section will be made freely available upon request.

3 Results and Discussion

The following results are all based on data set A. Note that all results are expressed in 'apparent mass', and to convert to static mass, Equation 3 can be used reformulated and used.

Acceleration events for a 5 minute long trip are identified as shown in Figure 2. Pane a) shows the entire trip for trial A)ii., and Pane b) shows a single acceleration event in detail for trial A)i. Both trips were controlled tests of the algorithms, and were meant to contain four explicit acceleration events. It is clear from Pane a) that many more accelerations were in fact captured, and Pane b) illustrates how steady-state mass estimates are obtained as the force and acceleration reach their asymptotic values.
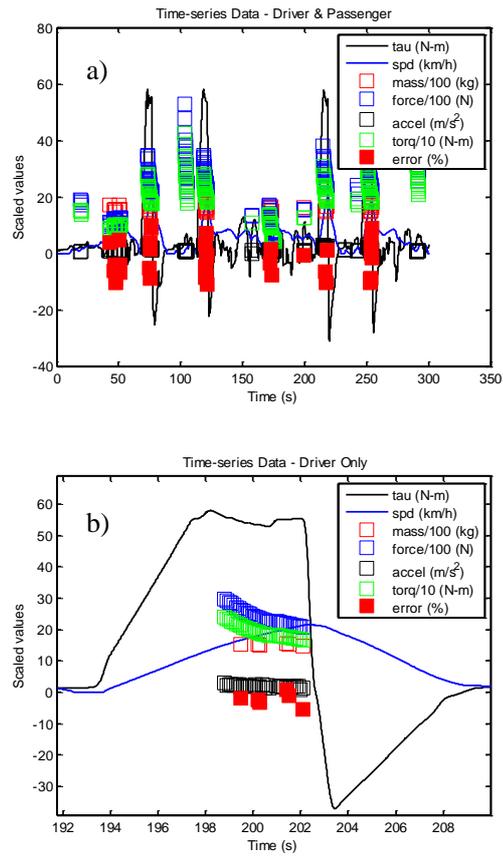

Figure 2: Mass identification using acceleration and torque. Pane a) an entire test run for A)ii. with 4 accelerations. Pane b) detail of the third acceleration event in trial A)i.

In step 8, the algorithm excludes events based on physical constraints. The limits are most often violated are outlined in Table 3, and for Trial A)ii. over 75% of all of the identified acceleration/torque events for which mass was calculated were excluded, mostly because they resulted in a physically impossible mass.

Table 3: Number of physical constraint violations for two trials

Trial	Accel.	Power	Torq.	Mass
A) i.	4	0	78	234
A) ii.	8	0	75	174

The implications of this exclusion step may be visualized clearly in Figure 3, where it can be seen that many identified masses do not conform basic physical constraints and can hence be safely excluded.

Filtered mass identification- Driver + Passenger
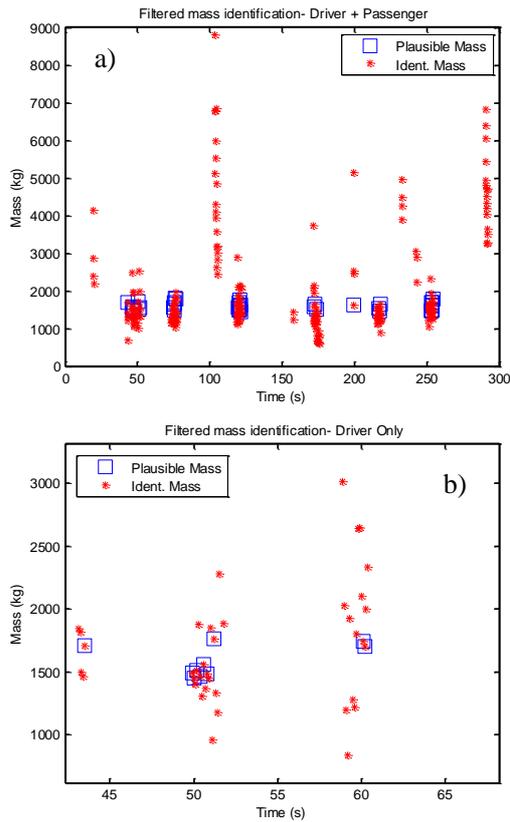

Filtered mass identification- Driver Only

Figure 3: Identified masses are parsed to plausible masses by filtering them through physical constraints. Pane a) all data for test A)ii. Pane b) zoomed in on one segment of test A)i.

The convergence of mass estimates using Equation 4 is shown in Figure 4. With an increasing number of measurements, the steady-state estimation for trial A)i. has a mean error of 2.3% and the trial A)ii. has a mean error of -2.4% as is shown in Figure 5.

Identified Mass - Driver Only
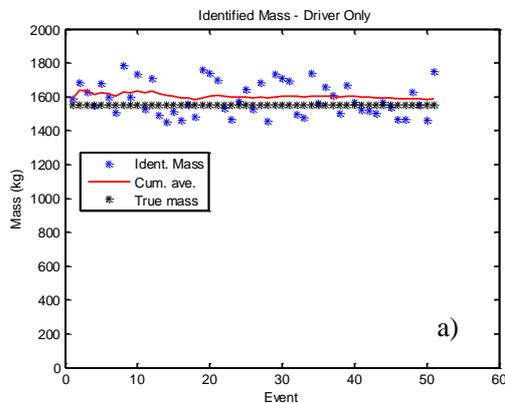

Identified Mass - Driver & Passenger
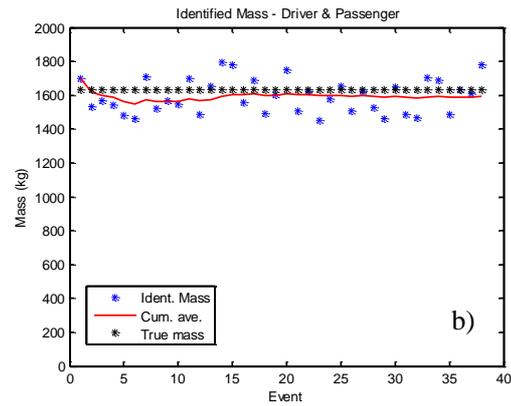
Figure 4: The mass for driver-only trial A)i. is slightly overestimated (2.3% error), and the mass for trial A)ii. is slightly underestimated (-2.7% error)

It is important to note that the variance for the error is high, at roughly +/-10% for both trials shown in Figure 5, and this has been identified as an area of future work. It is likely that this variance can be improved by applying a more complex approach to error minimization, for example by applying a minimum mean square error estimator.
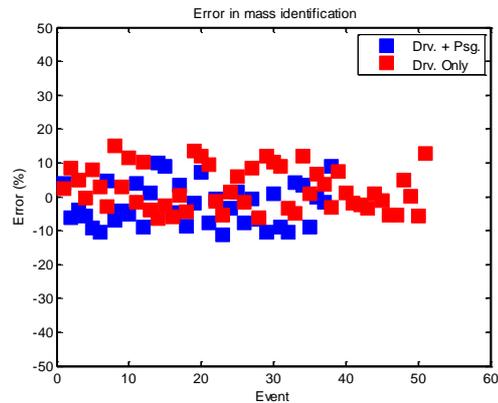

Error in mass identification

Figure 5: A high variance in the error is noted for both trial A)i. and trial A)ii.

3.1   Real-world driving

The results discussed in this short section are based on data from real-world driving collected in Set B which consists of long real-world trips (averaging 20 minutes) where no special attempts were made to do wide-open-throttle acceleration. No discernible difference between loaded and unloaded conditions as shown in Figure 6, where the mean identified mass for six trips are shown. It is hypothesized that while the added mass for the full condition is significant, without hard acceleration the current algorithm is confounded.
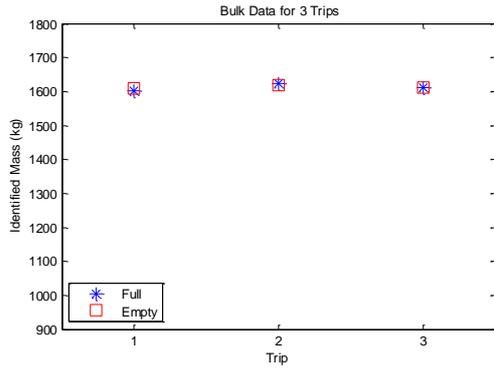
Figure 6: No perceivable difference in mass for long trips with real-world driving, as seen by plotting mean identified mass for 3 trips under condition B)i. (empty) and 3 trips under condition B)ii. (full)

3.2 Impact of mass on range

Many methods exist to predict electric vehicle 'distance to empty' (DTE) formulated in Equation 5, where E_b is the energy in the battery, and $\bar{p}_f$ is the mean consumption of the vehicle over a specific time interval.

$$D_{TE}(t) = \frac{E_b(t)}{\bar{p}_f(t)} \qquad (5)$$

They can be broadly classified as estimators based on previous consumption, and methods which try and predict route and energy consumption through physics-based models. To illustrate the importance of real-time mass estimation for electric vehicle range prediction, four methods are contrasted:

1. Plong – uses the mean power consumption over a long time window ($\bar{p}_f(t)$ averaged over 300km)
2. Pshort- uses a shorter time window ($\bar{p}_f(t)$ averaged over 30km)
3. Pblend – uses a blend of long/short $\bar{p}_f(t)$ averages (20/80 in this case)
4. Feedback – tracks actual DTE via a PI controller, and uses some smoothing factors to minimize driver startle
5. Pblend + model – uses the blended algorithm combined with the identified estimate of vehicle mass

Figure 7 shows how the various algorithms compare with one another. The method which incorporates a real-time estimate of vehicle mass

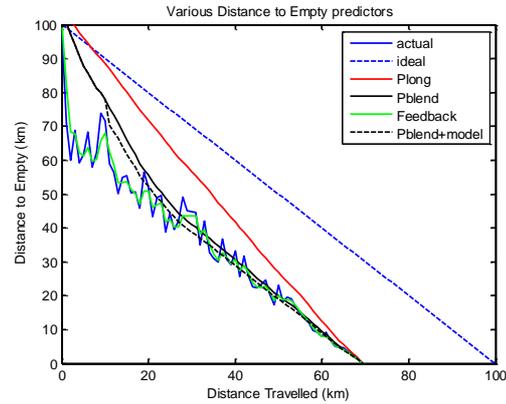performs the most accurately, after the feedback estimator.

Figure 7: comparison of distance to empty estimators, with a passenger joining at the 10 km mark.

While the error for the blended and modelled algorithm shown in Figure 8 is higher than for the 'Feedback' method, its dynamic characteristic seen in Figure 7 results in undesirable driver startle. This must be weighed against absolute error.
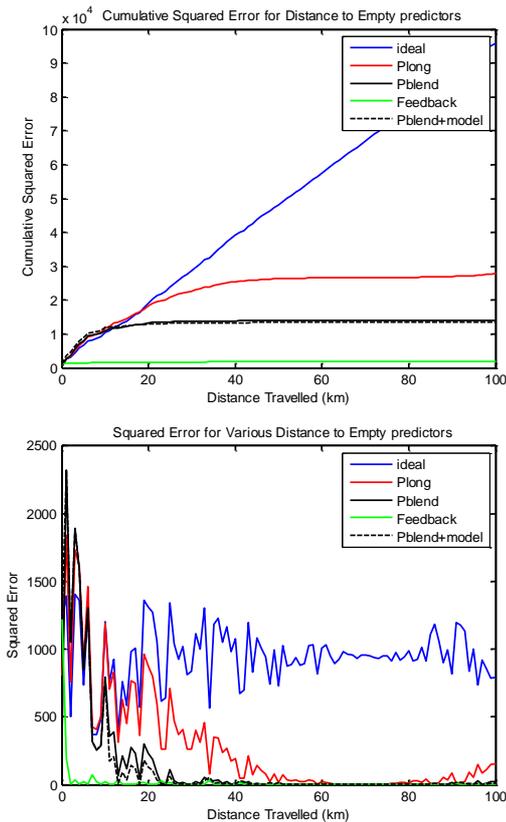

Figure 8: A comparison of the squared and cumulative squared error demonstrates the advantage of adding the model to the DTE estimate.

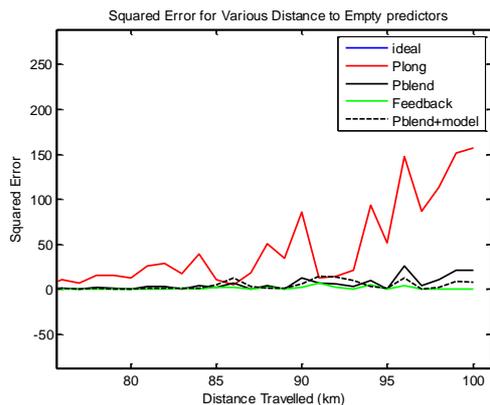The model adds useful precision, as seen in the zoomed perspective of Figure 9.

Figure 9: A detailed look at the last few km of the DTE highlighting the advantage of mass estimates.

4 Conclusions

The conclusions reached in this work are that:

1. Mass can be calculated to an acceptable accuracy in real-time using Newton's second law and efficient signal analysis,
2. For wide-open throttle events, mass can be estimated with +/- 3% accuracy,
3. For non-specific acceleration trials with real-world driving, algorithm accuracy degrades to +/- 10% (about +/- one passenger), and does not reach the level of accuracy required for individual passenger identification,
4. The application of real-time mass identification can substantially improve distance-to-empty estimates for EV's.

Acknowledgments

References

[1] J. M. Griffith and J. R. Venhuizen, "Least-squares estimates of automotive-drag coefficients from coast-down tests," presented at the American Control Conference, Seattle, WA, 1986.
[2] A. Vahidi, A. Stefanopoulou, and H. Peng, "Recursive Least Squares with Forgetting for Online Estimation of Vehicle Mass and Road Grade: Theory and Experiments," *Veh. Syst. Dyn.*, vol. 3, no. 1, 2005.
[3] H. S. Bae, J. Ryu, and C. Gerdes, "Road grade and vehicle parameter estimation for longitudinal control using GPS," presented at the Proceedings of IEEE Conference on Intelligent Transportation Systems, San Francisco, CA, 2001.
[4] B. L. Pence, "Recursive Parameter Estimation using Polynomial Chaos Theory Applied to Vehicle Mass Estimation for Rough Terrain," PhD Thesis, University of Michigan, Michigan, 2011.
[5] Erik Wilhelm, Lennon Rodgers, Raffaele Bornatico, and Gim Song Soh, "Towards Real-time Identification of Electric Vehicle Mass," presented at the APAC-17: Asia-Pacific Automotive Engineering Conference 2013, Bangkok, 2013.
[6] HP Wizard, "The Effects of Rotational Inertia on Automotive Acceleration." [Online]. Available: http://hpwizard.com/rotational-inertia.html. [Accessed: 12-Oct-2012].
[7] I. Preda, D. Covaciu, and G. Ciolan, "Coast Down Test - Theoretical and Experimental Approach," presented at the CONAT 2010 International Automotive Congress, Brasov, Romania, 2010.

Authors

Erik is an assistant professor at the Singapore University of Technology and Design (SUTD). He received his Honours BASc and MASc in Chemical Engineering from the University of Waterloo in 2005 and 2007 respectively, and his PhD from the ETH Zurich with Technology Assessment group at PSI in 2011. He performed post-doctoral research at the Massachusetts Institute of Technology before joining the SUTD.

Raffaele Bornatico received his MSc. degree in Mechanical Engineering in 2009 and his Dr. degree in 2012, both from ETH Zurich. He is part of the Institute for Dynamic Systems and Control. His research interests are in the area of dynamic system modeling and their application to solve real-world problems.

Lennon Rodgers received his PhD from MIT in 2013, as part of the MIT-SUTD International Design Center. He earned a B.S. from the University of Illinois Urbana/Champaign, and an M.S. from MIT. All of his degrees are in mechanical engineering. Before returning to MIT for graduate school, he worked at NASA's Jet Propulsion Laboratory and various technology companies.